DALTON

Molecules bearing a redox-active spacer. Synthesis and co-ordination behaviour of 1,1′-bis(5-methyl-2,5-diazahexyl)ferrocene

María José L. Tendero, Angel Benito, Ramón Martínez-Máñez * and Juan Soto

Departamento de Química, Universidad Politécnica de Valencia, Camino de Vera s/n, 46071 Valencia, Spain

New open-chain tetraamines containing ferrocene, 1,1′-bis(5-methyl-2,5-diazahexyl)ferrocene L^1 and 1,1′-bis(2,5-diazahexyl)ferrocene L^2, have been synthesized and characterized. Their protonation behaviour has been studied by potentiometric titrations in water (0.1 mol dm^{-3} KNO_3, 25 °C). The co-ordination ability of L^1 towards the divalent metal ions Ni^{2+}, Cu^{2+}, Zn^{2+}, Cd^{2+} and Pb^{2+} has also been studied. It forms both mono- and bi-nuclear complexes with Ni^{2+}, Cu^{2+}, Zn^{2+} and Cd^{2+} whereas only mononuclear species were found for Pb^{2+}. The electrochemical behaviour of L^1 has been studied in CH_2Cl_2 and water, $E_{\frac{1}{2}}$ is pH-dependent and from the $E_{\frac{1}{2}}$ *vs.* pH curve the protonation constants of oxidized L^1 (Fe^{III}) were determined. Similar electrochemical experiments were carried out for L^1–H^+–M^{2+} systems. The good agreement between the $E_{\frac{1}{2}}$ *vs.* pH and *z vs.* pH curves (*z* = average charge calculated from potentiometric data) appears to suggest that the ferrocene–substrate interaction is mainly electrostatic.

Redox-active groups have recently been employed for the synthesis of electroactive host molecules, which have proved useful in the electrochemical recognition of a large variety of substrates.[1] Electroactive moieties have been peripherally linked to ligands, used as building blocks in the synthesis of macrocycles or reported to act as a spacer linking two metal-binding domains. It has recently been reported that ferrocenyl units covalently anchored to polyamines are good candidates for the electrochemical recognition of transition-metal ions and anions in aqueous media.[2–4] These systems include polyamine bis(ferrocene) 'macrocycles', as in L^3,[2] and monoferrocene macrocycles where the polyaza chain is anchored to the two cyclopentadienyl rings in the same ferrocenyl unit.[3,4] The attachment of ferrocenyl units to polyamines produces pH- and redox-responsive molecules the electrochemical recognition properties of which can be enhanced or masked as a function of pH.[2] As a part of our interest in the use of redox-active molecules[5] we report here the synthesis of 1,1′-bis(5-methyl-2,5-diazahexyl)ferrocene L^1 and 1,1′-bis(2,5-diazahexyl)-ferrocene L^2 which are electroactive open-chain molecules containing a ferrocenyl group connecting two pH-responsive ethylenediamine moieties. Different frameworks have been used as spacers, the electronic and geometric properties of which along with those of the binding domains and metal ions determine the nature of the oligomer/polymers obtained.[6] Two specific properties are involved in the use of ferrocene as a spacer which are worthy of study and which are not normally found in other groups: (*i*) its ball-bearing like behaviour, due to the independent rotation of the two cyclopentadienyl rings;[7] and (*ii*) its electroactive character. Additionally, using ferrocene introduces some flexibility between the metal domains whilst retaining the possibility of electronic communication. The role of ferrocene as a ball-bearing spacer is studied by comparison of L^1 with the non-electroactive open-chain molecule L^5 and the electroactive cyclic polyamine L^3. We also report the protonation, co-ordination behaviour towards the divalent metal ions Ni^{2+}, Cu^{2+}, Zn^{2+}, Cd^{2+} and Pb^{2+} and electrochemical properties of L^1.

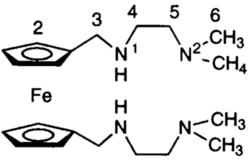

L^1

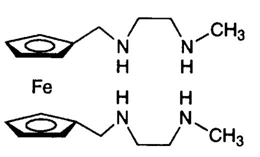

L^2

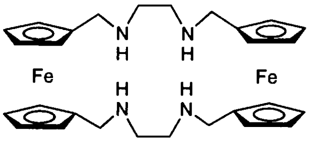

L^3

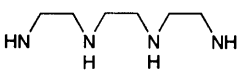

L^4

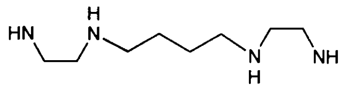

L^5

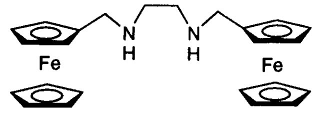

L^6

Experimental

Solvents and reagents

N,*N*-dimethyl- and *N*-methyl-ethane-1,2-diamine were of reagent quality used without further purification. Ferrocene-1,1′-dicarbaldehyde was synthesized following literature procedures.[8] Tetrahydrofuran (thf) was freshly distilled from sodium–benzophenone. Carbonate-free potassium hydroxide and hydrochloric acid solutions were used in the potentiometric and electrochemical experiments. Tetrabutylammonium perchlorate and potassium nitrate (0.1 mol dm^{-3}) were used as supporting electrolyte in dichloromethane and water, respectively.

Synthesis of L^1 and L^2

Ferrocene-1,1′-dicarbaldehyde (200 mg, 0.82 mmol) and *N*,*N*-dimethyl- or *N*-methyl-ethane-1,2-diamine (1.6 mmol) were heated to reflux in ethanol for 3 h. The solution was evaporated to dryness and the residue dissolved in dichloromethane (30 cm^3). Addition of hexane gave a red oil which was hydrogenated using $LiAlH_4$ (124 mg, 3.28 mmol) in freshly distilled thf (100 cm^3) at reflux for 1 h under argon. After careful addition of small amounts of water the mixture was filtered through Celite and the resulting solution evaporated to dryness. Basic water and dichloromethane were added and the organic phase was dried with anhydrous sodium sulfate, filtered and the yellow solution chromatographed on alumina by using dichloromethane–methanol (10:1) as eluent. Addition of hexane to the yellow band gave a yellow oil.

1,1′-Bis(5-methyl-2,5-diazahexyl)ferrocene (L^1) (200 mg, 63%) (Found: C, 62.2; H, 8.90; N, 14.45. $C_{20}H_{34}FeN_4$ requires C, 62.2; H, 8.80; N, 14.5%); NMR ($CDCl_3$); ^1H δ 4.14 (s, 4 H, C_5H_4), 4.06 (s, 4 H, C_5H_4), 3.50 (s, 4 H, CH_2), 2.69 (t, 4 H, CH_2), 2.40 (t, 4 H, CH_2) and 2.19 (s, 12 H, CH_3); ^{13}C δ 85.20 (C_{ipso}), 69.19 (C_5H_4), 68.63 (C_5H_4), 57.82 (CH_2), 48.26 (CH_2), 45.90 (CH_2) and 45.28 (CH_3).

1,1′-Bis(2,5-diazahexyl)ferrocene (L^2) (176 mg, 60%) (Found: C, 60.5; H, 8.45; N, 15.35. $C_{18}H_{30}FeN_4$ requires C, 60.4; H, 8.40; N, 15.65%): NMR ($CDCl_3$), ^1H δ 4.13 (s, 4 H, C_5H_4), 4.06 (s, 4 H, C_5H_4), 3.49 (s, 4 H, CH_2), 2.73 (t, 4 H, CH_2), 2.68 (t, 4 H, CH_2) and 2.41 (s, 6 H, CH_3); ^{13}C δ 87.10 (C_{ipso}), 72.84 (C_5H_4), 70.08 (C_5H_4), 58.08 (CH_2), 48.59 (CH_2), 45.95 (CH_2) and 45.09 (CH_3).

Physical measurements

The NMR spectra were measured on a Bruker AC-200 FT spectrometer operating at 300 K. Chemical shifts for ^1H and ^{13}C-{^1H} spectra are referenced to $SiMe_4$ and $CDCl_3$, respectively. Infrared spectra were taken on a Perkin-Elmer 1750 spectrophotometer as KBr pellets. Electrochemical data were obtained with a Tacusel IMT-1 programmable function generator, connected to a Tacusel PJT 120-1 potentiostat. The working electrode was platinum with a saturated calomel reference electrode (SCE) separated from the test solution by a salt bridge containing the solvent/supporting electrolyte. The auxiliary electrode was a platinum wire. Potentiometric titrations were carried out in water using a reaction vessel water-thermostatted at 25.0 ± 0.1 °C under nitrogen. The titrant was added by a Crison microburete 2031. The measurements were made using a Crison 2002 pH-meter and a combined glass electrode. The titration system was automatically controlled by a personal computer using a program which monitors the electromotive force and the volume of titrant added. The electrode was calibrated as a hydrogen-concentration probe by titration of well known amounts of HCl with CO_2-free KOH solution and determining the equivalence point by Gran's method[9] which gives the standard potential E'° and the ionic product of water ($K'_w = [H^+][OH^-]$). The logarithm of K'_w for the solvent used was found to be −13.7 ± 0.1 (25 °C, 0.1 mol dm^{-3} KNO_3). The concentrations of the nickel(II), copper(II), zinc(II), cadmium(II) and lead(II) solutions were determined using standard methods. The computer program SUPERQUAD[10] was used to calculate the protonation and stability constants. The titration curves for each system (about 200 experimental points corresponding to at least three titration curves, range pH = −log[H] 2.5–10, ligand concentration *ca.* 1.2×10^{-3} mol dm^{-3}, metal concentration 2.5×10^{-3}–0.5×10^{-3} mol dm^{-3} according to the formation of mono- and di-nuclear species) were treated either as a single set or as separate entities without significant variations in the values of the stability constants. The sets of data were merged and treated simultaneously to give the stability constants.

Results and Discussion

Reaction of *N,N*-dimethyl- or *N*-methyl-ethane-1,2-diamine with ferrocene-1,1′-dicarbaldehyde yields the Schiff-base derivatives 1,1′-bis(5-methyl-2,5-diazahex-1-enyl)- or 1,1′-bis(2,5-diazahex-1-enyl)-ferrocene, respectively. These compounds are oils and have always been obtained impure with small amounts of starting materials, no further attempt was made to purify them. Their ^1H NMR spectra show a total of six resonances; two for the α- and β-protons in the ferrocenyl framework, two for the non-equivalent CH_2 groups, one for the CH_3 moiety and a characteristic signal at δ 8.16 attributed to the presence of an imino group. Hydrogenation of them using $LiAlH_4$ in thf resulted in the corresponding tetraamines L^1 and L^2. The main feature in the ^1H NMR spectra of L^1 and L^2 when compared with those of their precursors is the lack of the low-field imino proton and the existence of a new signal at δ 3.50 attributed to the CH_2 groups nearest to the ferrocenyl group.

Compounds L^1 and L^2 are soluble in organic solvents but are also water soluble due to the presence of amino groups. Both can only be obtained as oils, and all our attempts to isolate them as solids were unsuccessful. Aqueous saturated solutions of L^1 and L^2 can be prepared by boiling them in distilled water overnight to produce bright yellow solutions the concentrations of which were determined by iron analysis; L^1 is more soluble than L^2 in water. Typical concentrations were 1.2×10^{-3} and 2.0×10^{-4} mol dm^{-3} for L^1 and L^2, respectively.

Protonation behaviour

The behaviour of L^1 and L^2 towards protonation was studied by potentiometric titrations with KOH for previously acidified solutions in water (0.1 mol dm^{-3} KNO_3) at 298.1 ± 0.1 K. Table 1 lists the basicity constants of L^1 and L^2 together with those of the tetraamines 2,5,19,22-tetraaza[6.6](1,1′)ferrocenophane (L^3),[2] 3,6-diazaoctane-1,8-diamine (L^4)[11] and 3,8-diazadecane-1,10-diamine (L^5).[11,12] Fig. 1 shows the distribution diagram of L^1. When open-chain polyamines L^1 and L^2 are compared with the analogous cyclic one L^3 it can be noticed that, although a different solvent medium has been used for determining the basicity constants, L^3 behaves as a stronger acid than L^1 and L^2. This appears to agree with the cyclic nature of L^3. The free rotation around the cylopentadienyl rings which can easily occur in L^1 and L^2 but not in L^3 minimizes the effect of the charge repulsions between ammonium groups.

The difference between the first two protonation constants for L^1 is 0.9 logarithm unit, whereas the difference Δ(log *K*) between the values of the second and third steps is about 2 and between the third and the fourth is 1.2. The small difference between the first two suggests that, after the first protonation, the second proton attacks the arm in L^1 which is unprotonated. The third and the fourth protons should be placed near two already protonated nitrogens separated by ethylenic chains, and therefore are less basic than the first two protons leading to a higher Δ(log *K*)

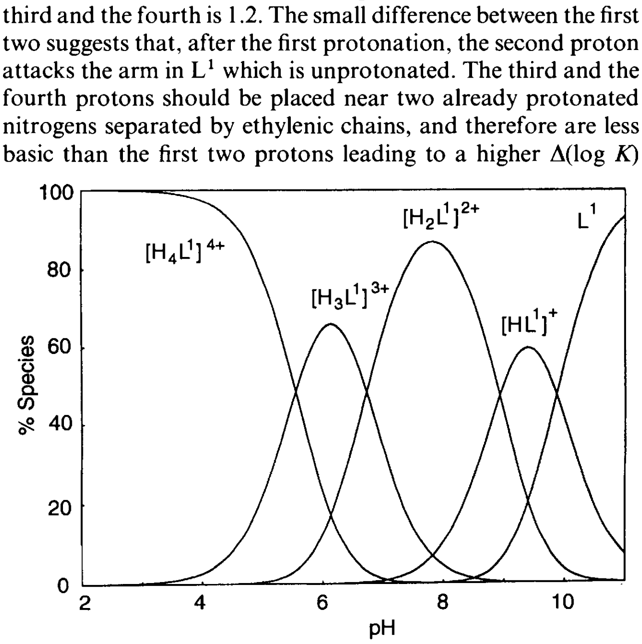

Fig. 1 Distribution diagram for the L^1–H^+ system as a function of pH

Table 1 Stepwise protonation constants (log *K*) of L^1 and L^2 determined in water at 25 °C in 0.1 mol dm^{-3} KNO_3

Reaction[a]	L^1 log *K*	L^1 Δlog *K*	L^2 log *K*	L^2 Δlog *K*	L^3 (ref. 2)	L^4 (ref. 11)	L^5 (ref. 11)
$L + H \rightleftharpoons HL$	9.87(3)[b]		9.59(3)		8.40	9.74(6)	10.44(4)
$HL + H \rightleftharpoons H_2L$	8.93(2)	0.94	9.06(3)	0.53	6.71	9.07(3)	9.71(3)
$H_2L + H \rightleftharpoons H_3L$	6.72(3)	2.21	7.15(2)	1.91	5.15	6.59(3)	7.64(4)
$H_3L + H \rightleftharpoons H_4L$	5.55(3)	1.17	5.11(3)	2.04	2.45	3.27(7)	6.83(3)

[a] Charges have been omitted for clarity. [b] Values in parentheses are standard deviations on the last significant figure.

There is good agreement between the first three basicity constants of L^1, L^4 and L^5 whereas for the last protonation constant the agreement is still good for L^1 and L^5 but in L^4 the last proton is much more acidic. For L^4 the last protonation takes place on one of the central ethylenic nitrogens which is separated from the adjacent ammonium groups by two ethylenic chains, whereas for L^1 and L^5 the distance between the last nitrogen to be protonated and one of the adjacent ammonium groups is at least increased by $-CH_2-Fe(C_5H_4)_2-CH_2-$ and $-(CH_2)_4-$ spacers with a corresponding decrease in charge repulsion. As expected and as observed, this is in accord with the fact that the presence of larger spacers between nitrogens yields higher basicity than does shorter ones.[13] The protonation constants found for the molecule L^2 are similar to those of L^1. However, the low solubility of L^2 in water ($c = 2.0 \times 10^{-4}$ mol dm^{-3}) prevents a further detailed study of its protonation, metal co-ordination and electrochemical behaviour.

To perform a more detailed study of the protonation of L^1 we recorded its ^{13}C-{^1H} NMR spectra at different pH values. Throughout the pH range studied the number of ^{13}C signals was independent of pH. Resonances at δ 76.69 and 75.89 (pH 10) are attributed to the α- and β-carbons in the ferrocenyl groups. The signals in the range δ 64.23–51.83 are assigned to the three non-equivalent CH_2 groups, whereas a resonance at δ 51.07 is attributed to the CH_3 moieties. The assignment of all the signals was confirmed (HETCOR) by two-dimensional heteronuclear correlation ^1H–^{13}C experiments. Carbons C^1–C^3 and C^6 only suffer a slight variation of the chemical shift, whereas C^4 and C^5 are more affected by protonation (see Fig. 2). In the range pH 10–9 where the two first protons attack the molecule, no variation in the chemical shift of C^4 occurs, but an upfield shift of the signal assigned to carbon C^5 takes place. Taking into account that C^5 is located in β position to the nitrogen N^1, these variations suggest that the first two protonations would mainly affect the two secondary nitrogens nearest to the ferrocenyl spacer. In the range pH 9–5 where the next two protonations occur the most significant feature is the upfield shift of C^4, which seems to confirm that the terminal tertiary nitrogens are mainly involved in the last two protonation steps.

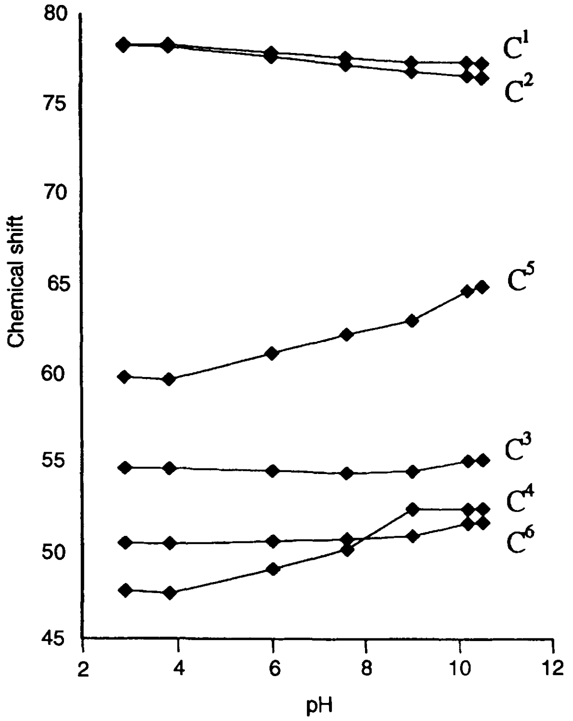

Fig. 2 Plots of the ^{13}C NMR chemical shifts of the amine L^1 as a function of pH

Metal co-ordination

Table 2 lists the stability constants for the formation of complexes of L^1 with the divalent metal ions Ni^{2+}, Cu^{2+}, Zn^{2+}, Cd^{2+} and Pb^{2+}, Table 3 those of L^5 with Ni^{2+}, Cu^{2+}, Zn^{2+} and Cd^{2+} taken from refs. 11 and 12.

Compound L^1 forms both mono- and bi-nuclear complexes with the metal ions studied. The values of the stability constants for the formation of the $[ML]^{2+}$ species are lower for L^1 than for L^5 with decreases in stability of 7.1, 7.9, 4.3 and 4.6 logarithmic units for the complexes of Ni^{2+}, Cu^{2+}, Zn^{2+} and Cd^{2+}, respectively. The logarithms of the constants for the first protonation step $[ML^1]^{2+} + H^+ \rightleftharpoons [M(HL^1)]^{3+}$ and for the second protonation $[M(HL^1)]^{3+} + H^+ \rightleftharpoons [M(H_2L^1)]^{4+}$ of the complexes of Ni^{2+}, Cu^{2+}, Zn^{2+} and Cd^{2+} are higher than those for the third, $[H_2L^1]^{2+} + H^+ \rightleftharpoons [H_3L^1]^{3+}$, and fourth protonation, $[H_3L^1]^{3+} + H^+ \rightleftharpoons [H_4L^1]^{4+}$, of free L^1. For L^5 the situation is quite different. The $[ML^5]^{2+}$ complexes (M = Ni^{2+}, Cu^{2+}, Zn^{2+} or Cd^{2+}) show first and second protonation constants lower than the third and fourth protonation constants of the free amine L^5, suggesting, in contrast with L^1 a M–N cleavage process upon protonation. Although precise information on co-ordination numbers cannot be deduced from the values of the stability constants, the study suggests that with L^1 the number of nitrogens co-ordinated in the $[ML^1]^{2+}$ complexes of Ni^{2+}, Cu^{2+}, Zn^{2+} and Cd^{2+} is less than with L^5. Therefore we may assume that for 1 : 1 complexes co-ordination takes place mainly in mode **I** rather than **II** for these metal ions. This is also supported by the fact that species of stoichiometry 1 : 2 (metal : ligand) are found in solution containing metal to ligand ratios of 1 : 1 as shown in the distribution diagram of the L^1–H^+–Cd^{2+} system (Fig. 3). For L^6 the logarithm of the constant for the process $L + Cu^{2+} \rightleftharpoons [CuL]^{2+}$ is 9.77(1). The similar value found for L^1 for the same process suggests once again co-ordination mode **I**.

For compound L^3 the logarithms of the constants for the first protonation step $[ML^3]^{2+} + H^+ \rightleftharpoons [M(HL^3)]^{3+}$, are 4.8, 5.9 and 6.1 for Cu^{2+}, Ni^{2+} and Zn^{2+}, respectively,[2] whereas the logarithm of the constant for the third protonation of free L^3, $[H_2L^3]^{2+} + H^+ \rightleftharpoons [H_3L^3]^{3+}$, is 5.2. These data suggest, at least for Ni^{2+} and Zn^{2+}, that the number of nitrogens involved in the co-ordination of these metal ions is, as for L^+, less than four. The ferrocene group in L^1 and L^3 does not

Table 2 Stability constants (log *K*) for the formation of complexes of Ni^{2+}, Cu^{2+}, Zn^{2+}, Cd^{2+} and Pb^{2+} with L^1 in water 25 °C in 0.1 mol dm^{-3} KNO_3

Reaction[a]	Ni^{2+}	Cu^{2+}	Zn^{2+}	Cd^{2+}	Pb^{2+}
$M + L + 2H \rightleftharpoons M(H_2L)$	21.38(3)[b]	24.34(1)	22.29(2)	21.14(4)	—
$M + L + H \rightleftharpoons M(HL)$	14.85(2)	18.50(2)	14.84(2)	13.59(3)	14.12(2)
$M + L \rightleftharpoons ML$	5.31(3)	11.38(2)	6.14(2)	4.39(2)	7.15(1)
$2M + L \rightleftharpoons M_2L$	9.82(2)	16.15(2)	9.38(2)	7.72(3)	—
$M + L + H_2O \rightleftharpoons ML(OH) + H$	—	—	—	—	−1.92(4)
$2M + L + 2H_2O \rightleftharpoons M_2L(OH)_2 + 2H$	−8.55(3)	2.29(2)	−5.45(2)	−11.27(3)	—
$M + ML \rightleftharpoons M_2L$	4.51	4.77	3.24	3.33	—
$H + ML \rightleftharpoons M(HL)$	9.54	7.12	8.70	9.2	6.97
$H + M(HL) \rightleftharpoons M(H_2L)$	6.53	5.84	7.45	7.55	—
$M_2L + 2H_2O \rightleftharpoons M_2L(OH)_2 + 2H$	−18.37	−13.86	−14.83	−18.99	—

[a] Charges have been omitted for clarity. [b] Values in parentheses are standard deviations on the last significant figure.

Table 3 Stability constants (log *K*) for the formation of complexes of Ni^{2+}, Cu^{2+}, Zn^{2+} and Cd^{2+} with L^5 in water at 25 °C in 1 mol dm^{-3} KNO_3[a]

Reaction[b]	Ni^{2+}	Cu^{2+}	Zn^{2+}	Cd^{2+}
$M + L + 2H \rightleftharpoons M(H_2L)$	24.57	27.52	22.92	23.07
$M + L + H \rightleftharpoons M(HL)$	18.57	23.42	16.27	16.02
$M + L \rightleftharpoons ML$	12.38	19.34	9.80	8.95
$2M + L \rightleftharpoons M_2L$	13.68	—	—	11.15
$M + ML \rightleftharpoons M_2L$	1.3	—	—	2.2
$H + ML \rightleftharpoons M(HL)$	6.19	4.08	6.47	7.07
$H + M(HL) \rightleftharpoons M(H_2L)$	6.0	4.1	6.65	7.05

[a] Data taken from ref. 11. [b] Charges have been omitted for clarity.

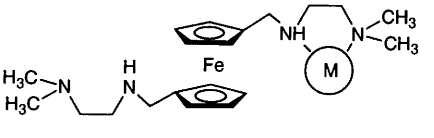

mode I

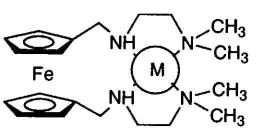

mode II

Table 4 Electrochemical data[a]

Compound	$E_{p_a}{}^b$/V
L^1	0.48(74)
L^2	0.47(75)

[a] Obtained in dichloromethane, 0.1 mol dm^{-3} $[NBu^n{}_4][PF_6]$ as supporting electrolyte at 25 °C. Platinum as electrode. Potentials were determined with reference to the SCE. [b] Anodic peak potential. Values in parentheses are the differences between the anodic and cathodic peak potentials in mV.

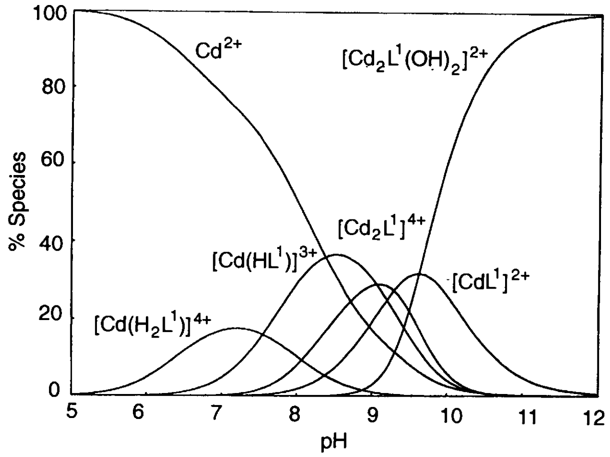

Fig. 3 Distribution diagram for the L^1–H^+–Cd^{2+} system as a function of pH. Ratio L^1: Cd^{2+} = 1 : 1

appear to favour the co-ordination of all the N donor atoms. This is probably due to some constraints imposed by ferrocene related to the existence of coplanar cyclopentadienyl (cp) rings with an invariable cp · · · cp distance.

If the stability constants of the $[ML^1]^{2+}$ species were in accord with the Irving–Williams order they should be in the sequence $Ni^{2+} < Cu^{2+} > Zn^{2+} > Cd^{2+} > Pb^{2+}$. The data we have obtained for L^1 is consistent with this except for Pb^{2+} which shows a stability constant for the $[PbL^1]^{2+}$ complex higher than that with Ni^{2+}, Zn^{2+} and Cd^{2+}. This high stability constant along with the lack of $[M(H_2L^1)]^{4+}$ species may be explained assuming that co-ordination mode **II** is more favourable for metal ions with large cationic radii. In fact Pb^{2+} shows not only a lower stability constant for the process $[ML^1]^{2+} + H^+ \rightleftharpoons [M(HL^1)]^{3+}$, but its value is also similar to that found for the third protonation step of free L^1.

Another noticeable difference between the co-ordination behaviour of L^1 and L^5 is that the former forms binuclear complexes with Ni^{2+}, Cu^{2+}, Zn^{2+} and Cd^{2+}, whereas for L^5 the formation of binuclear species was found for Ni^{2+} and Cd^{2+}. The lack of binuclear species and low stability constants for the process $M + ML \rightleftharpoons M_2L$ with Ni^{2+} and Cd^{2+} is consistent with the fact that co-ordination of a second metal ion to L^5 would involve cleavage of M–N bonds. The existence of binuclear complexes with higher stability constants for this process with L^1 than with L^5 may reflect again the low co-ordination number achieved with L^1 when compared to L^5.

Electrochemical study

The electrochemical data for compounds L^1 and L^2 in CH_2Cl_2 ($[NBu^n{}_4][PF_6]$ as supporting electrolyte) are summarized in Table 4. The compounds display reversible oxidation processes with a separation of about 80 mV and with anodic and cathodic intensity ratios close to unity. Plots of i_p *versus* $v^{\frac{1}{2}}$ (from cyclic voltammetry experiments; i_p = anodic peak intensity and v = scan rate) indicate that the electrochemical oxidation is controlled by diffusion. However the corresponding Schiff-base derivatives 1,1′-bis(5-methyl-2,5-diazahex-1-enyl)- or 1,1′-bis(2,5-diazahex-1-enyl)-ferrocene show an irreversible oxidation process at 0.71 V *versus* SCE in contrast with other related Schiff-base ferrocene-containing derivatives which exhibit

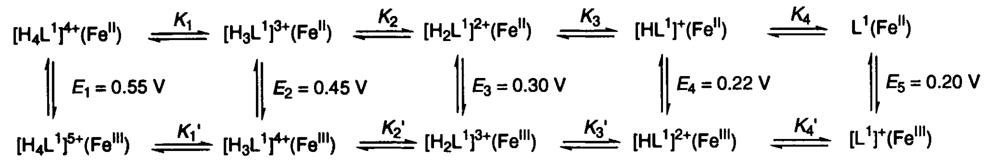

Scheme 1

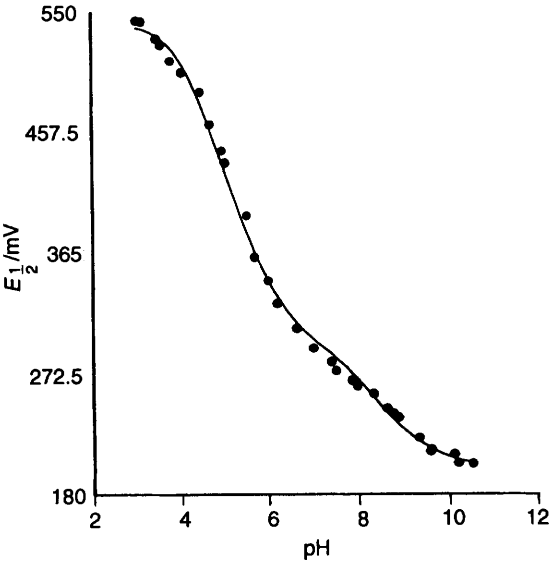

Fig. 4 Plot of the half-wave potential ($E_{\frac{1}{2}}$) *versus* pH for L^1 showing the fit using equation (1)

reversible or quasi-reversible oxidation processes.[5] When the Schiff-base derivatives are chemically transformed into L^1 and L^2 the oxidation peak potential is shifted by 230 mV on account of the transformation of the imino to amino moieties.

We have also studied the electrochemical behaviour of L^1 in water under the same conditions at which the potentiometric measurements were carried out. The oxidation potential of L^1 in water is pH-dependent. A plot of the half-wave potential from rotating disc electrode experiments ($E_{\frac{1}{2}}$) *versus* pH is shown in Fig. 4; $E_{\frac{1}{2}}$ changes from 204 mV at pH 10 to 543 mV at pH 3 with a total $\Delta E_{\frac{1}{2}}$ increment due to the attachment of four protons to L^1 of 339 mV. Molecule L^3 gives an $\Delta E_{\frac{1}{2}}$ of 239 mV (tetrahydrofuran–water, 70:30 v/v; pH 2–10). Taking into account the equilibria shown in Scheme 1, equation (1)[2,14] should fit the curve in Fig. 4. Here $E^\circ_{\frac{1}{2}}$ is the half-wave potential of the couple $[H_4L^1]^{4+}(Fe^{II})$–$[H_4L^1]^{5+}(Fe^{III})$ at pH 0 and K_n, K_n' are the acid-dissociation constants of the 'reduced' and oxidized species, respectively. Table 5 gives the stepwise protonation constants for the oxidized species $[H_jL^1]^{(j+1)+}(Fe^{III})$ (K_n') obtained by fitting the curve of $E_{\frac{1}{2}}$ *versus* pH using equation (1).

$$E = E^\circ_{\frac{1}{2}} + \frac{RT}{nF}\ln\frac{a_{red}}{a_{ox}} \tag{1}$$

$$a_{red} = K_1K_2K_3K_4 + K_1K_2K_3[H^+] + K_1K_2[H^+]^2 + K_1[H^+]^3 + [H^+]^4 \tag{2}$$

$$a_{ox} = K_1'K_2'K_3'K_4' + K_1'K_2'K_3'[H^+] + K_1'K_2'[H^+]^2 + K_1[H^+]^3 + [H^+]^4 \tag{3}$$

The ferrocenyl group is an electroactive spacer and it can be switched by electric energy from neutral to a positively charged ferrocenium group. This switching process induces the $[H_jL^1]^{(j+1)+}(Fe^{III})$ species to be more acidic than the corresponding 'reduced' $[H_jL^1]^{j+}(Fe^{II})$ ones. This is consistent with the presence of an extra charge on the oxidized iron(III) molecule which creates additional charge repulsions between the ammonium groups and the ferrocenium moiety.

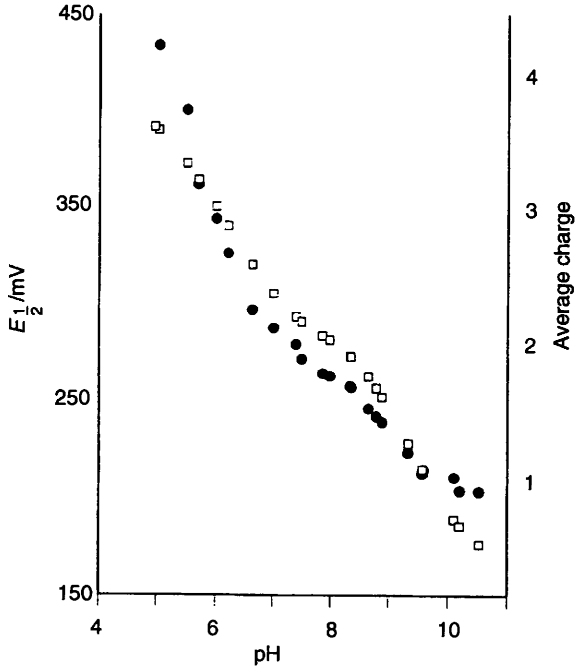

Fig. 5 Plots of $E_{\frac{1}{2}}$ *vs.* pH (●) and *z vs.* pH (☐) for the system L^1–H$^+$

Table 5 Stepwise protonation constants of L^1 (Fe^{III}) at 25 °C

Reaction[a]	log *K*[b]
$L(Fe^{III}) + H \rightleftharpoons HL(Fe^{III})$	9.5(1)
$HL(Fe^{III}) + H \rightleftharpoons H_2L(Fe^{III})$	7.7(1)
$H_2L(Fe^{III}) + H \rightleftharpoons H_3L(Fe^{III})$	4.2(1)
$H_3L(Fe^{III}) + H \rightleftharpoons H_4L(Fe^{III})$	3.8(1)

[a] Charges have been omitted for clarity. [b] Values in parentheses are standard deviations on the last significant figure.

The difference between the first protonation constants of the 'reduced' L^1(Fe^{II}) and oxidized L^1(Fe^{III}) species is 0.4 log units, that between the second protonation constants is 1.2 log units and those between the third and the fourth protonation constants are 2.5 and 1.7. The fact that the first and the second constants are quite similar for L^1(Fe^{II}) and L^1(Fe^{III}) suggests that the first two protonations in L^1(Fe^{III}) would affect the two tertiary nitrogens furthest from the ferrocenium group. The last two protonations would then mainly affect the secondary nitrogens nearest the oxidized spacer. This protonation model is different to that found for the 'reduced' L^1(Fe^{II}) molecule, where the first two protonations occur at the two secondary nitrogens nearest the ferrocene moiety. However it seems reasonable that the presence of a positive charge in the centre of the molecule would produce a different protonation model in the oxidized L^1(Fe^{III}) molecule.

We have recently reported[15] that in some cases the curve of $E_{\frac{1}{2}}$ *versus* pH can adequately be simulated by plotting the average charge (z) *versus* pH. Average charge is defined as $z = \Sigma x_i z_i$ where z_i and x_i are the charge and the molar fraction for

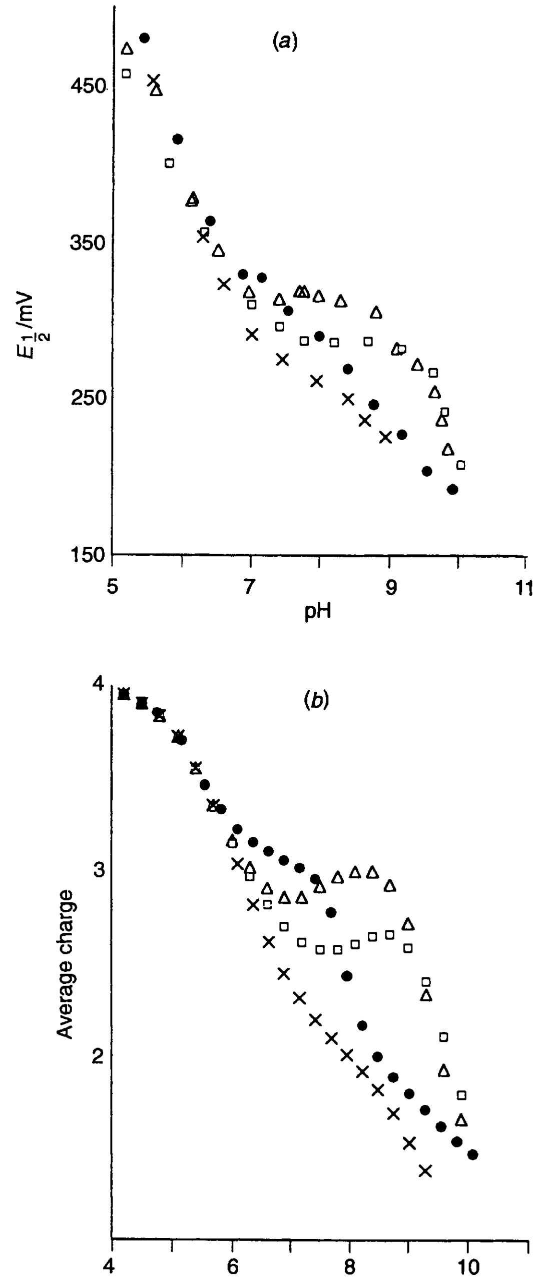

Fig. 6 Plots *vs.* pH of (*a*) the half-wave potential ($E_{\frac{1}{2}}$) and (*b*) average charge *z* for L^1-H^+-M^{2+} calculated from potentiometric data [M = Ni (△), Zn (●), Cd (□) or Pb (X)]

the *i*th electroactive species; x_i can easily be calculated from the potentiometric data. Fig. 5 shows a comparison between the experimental $E_{\frac{1}{2}}$ *vs.* pH curve and the *z vs.* pH curve for L^1. There is good agreement in the range pH 5–10 between the experimental and calculated curves although the similarity is not good at pH < 5. Fig. 6(*a*) shows the variation of $E_{\frac{1}{2}}$ *versus* pH for a 1 : 1 molar ratio mixture of L^1 and Ni^{2+}, Zn^{2+}, Cd^{2+} and Pb^{2+}. At pH < 6.5 the $E_{\frac{1}{2}}$ values for the L^1-H^+ and L^1-H^+-M^{2+} systems are nearly the same (Cu^{2+} shows a similar behaviour but is not included in Fig. 6 for clarity), whereas at pH > 6.5 the presence of these metals shifts the ferrocenyl half-wave potential to cathodic potentials when compared to that of free L^1. The fact that different metals cause a different shift in the oxidation potential of the ferrocenyl groups is basic in the design of potential electrochemical sensors based on pH-responsive redox-active molecules. As can be seen there is a good agreement between Fig. 6(*a*) and 6(*b*) which shows a plot of the average charge (calculated from potentiometric data) *versus* pH. Similar results were obtained using other pH-responsive redox-active molecules such as *N,N′,N″,N‴*-tetrakis(4-ferrocenyl-3-azabutyl)-1,4,8,11-tetraazacyclotetradecane.[15] Therefore, although it has to be pointed out that we have found that there is not always a good agreement between the experimental $E_{\frac{1}{2}}$ *vs.* pH and calculated *z vs.* pH curves, the present data suggest that the ferrocene–substrate interaction is mainly electrostatic in these systems. This is in agreement with some recent results[16] showing a linear relation between the shift of the redox potentials and the inverse of the iron–nitrogen distance in similar ferrocene-containing amines. In fact, compounds related to L^2, such as L^3 and L^6, show a shift of $E_{\frac{1}{2}}$ between the free compound and the fully protonated species $[H_4L^3]^{4+}$ and $[H_4L^6]^{4+}$ of 238 and 128 mV, respectively with crystallographic data showing shorter iron–nitrogen distances for L^3 (3.509 Å)[2] than for L^6 (4.435 Å)[5] in line with an electrostatic Coulomb model.

References

1 See, for example, T. Saji and I. Kinoshita, *J. Chem. Soc., Chem. Commun.*, 1986, 716; J. C. Medina, T. T. Goodnow, S. Batt, J. L. Atwood, A. E. Kaifer and G. W. Gokel, *J. Chem. Soc., Chem. Commun.*, 1991, 290; J. C. Medina, I. Gay, Z. Chen, L. Echegoyen, and G. W. Gokel, *J. Am. Chem. Soc.*, 1991, **113**, 365; C. D. Hall, J. H. R. Tucker and N. W. Sharpe, *Organometallics*, 1991, **10**, 1727; P. D. Beer, J. P. Danks, D. Hesek and J. F. McAleer, *J. Chem. Soc., Chem. Commun.*, 1993, 1735; P. D. Beer, D. B. Crowe, M. I. Ogden, M. G. B. Drew and B. Main, *J. Chem. Soc., Dalton Trans.*, 1993, 2107; C. D. Hall, J. H. R. Tucker, S. Y. F. Chu, A. W. Parkins and S. C. Nyborg, *J. Chem. Soc., Chem. Commun.*, 1993, 1505; P. D. Beer, D. Hesek, J. E. Kingston, D. K. Smith, S. E. Stokes and M. G. B. Drew, *Organometallics*, 1995, **14**, 3288; A. Ori and S. Shinkai, *J. Chem. Soc., Chem. Commun.*, 1995, 1771; C. Dusemund, K. R. A. Samankumara Sandanakaye and S. Shinkai, *J. Chem. Soc., Chem. Commun.*, 1995, 333.

2 M. J. L. Tendero, A. Benito, R. Martínez-Máñez, J. Soto, J. Payá, A. J. Edwards and P. R. Raithby, *J. Chem. Soc., Dalton Trans.*, 1996, 343.

3 P. D. Beer, Z. Chen, M. G. B. Drew, J. Kingston, M. Ogden and P. Spencer, *J. Chem. Soc., Chem. Commun.*, 1993, 1046.

4 M. J. L. Tendero, A. Benito, J. M. Lloris, R. Martínez-Máñez, J. Soto, J. Payá, A. J. Edwards and P. R. Raithby, *Inorg. Chim. Acta*, 1996, **247**, 139.

5 A. Benito, J. Cano, R. Martínez-Máñez, J. Soto, J. Payá, F. Lloret, M. Julve, J. Faus and M. D. Marcos, *Inorg. Chem.*, 1993, **32**, 1197; A. Benito, J. Cano, R. Martínez-Máñez, J. Payá, J. Soto, M. Julve, F. Lloret, M. D. Marcos and E. Sinn, *J. Chem. Soc., Dalton Trans.*, 1993, 1999; J. Cano, A. Benito, R. Martánez-Máñez, J. Soto, J. Payá, F. Lloret, M. Julve, M. D. Marcos and E. Sinn, *Inorg. Chim. Acta*, 1995, **231**, 45; M. J. L. Tendero, A. Benito, J. Cano, J. M. Lloris, R. Martínez-Máñez, J. Soto, A. J. Edwards, P. R. Raithby and M. A. Rennie, *J. Chem. Soc., Chem. Commun.*, 1995, 1643.

6 F. Vögtle, *Supramolecular Chemistry*, Wiley, Chichester, 1991; E. C. Constable, A. M. W. Cargill Thompson and D. A. Tocher, in *Supramolecular Chemistry*, ed. V. Balzani, NATO ASI Series, Reidel, Dordrecht, 1992; E. C. Constable, *Prog. Inorg. Chem.*, 1994, **42**, 67.

7 E. C. Constable, A. J. Edwards, M. D. Marcos, P. R. Raithby, R. Martínez-Máñez and M. J. L. Tendero, *Inorg. Chim. Acta*, 1994, **224**, 11; J. C. Medina, C. Li, S. G. Bott, J. L. Atwood and G. W. Gokel. *J. Am. Chem. Soc.*, 1991, **113**, 366.

8 G. G. A. Balavoine, G. Doisneau and T. Fillebeen-Khan, *J. Organomet. Chem.*, 1991, **412**, 381.

9 G. Gran, *Analyst* (*London*), 1952, **77**, 661; F. J. Rossotti and H. J. Rossotti, *J. Chem. Educ.*, 1965, **42**, 375.

10 P. Gans, A. Sabatini and A. Vacca, *J. Chem. Soc., Dalton Trans.*, 1985, 1195.

11 R. M. Smith and A. E. Martell, *Critical Stability Constants*, Plenum, New York, vol. 6.

12 G. Anderegg and P. Blauenstein, *Helv. Chim. Acta*, 1982, **65**, 913.

13 R. D. Hancock and A. E. Martell, *Comments Inorg. Chem.*, 1988, **6**, 237; J. A. Aguilar, A. Bianchi, E. García-España, S. V. Luis, J. M. Llinares, J. A. Ramirez and C. Soriano., *J. Chem. Soc., Dalton Trans.*, 1994, 637.

14 W. M. Clark, in *Oxidation-Reduction Potentials of Organic Systems*, Williams & Wilkins Co., Baltimore, MD, 1960; M. Haga, T. Ano, K. Kano and S. Yamabe, *Inorg. Chem.*, 1991, **30**, 3843; M. Haga, T. Ano, T. Ishizaki, K. Kano, K. Nozaki and T. Ohno, *J. Chem. Soc., Dalton Trans.*, 1994, 263.

15 M. J. L. Tendero, A. Benito, R. Martínez-Máñez, J. Soto, E. García-España, J. A. Ramírez, M. I. Burguete, S. V. Luis, *J. Chem. Soc., Dalton Trans.*, 1996, 2923.

16 H. Plenio, J. Yang, R. Diodone and J. Heinze, *Inorg. Chem.*, 1994, **33**, 4098.

Received 11*th March* 1996; *Paper* 6/01703G